An ALE Finite Element Formulation and Fractional Step Method to Solve Fluid-Structure Interaction Problems with Modified Laplacian Equation for Mesh Movement

Alessandro R. E. Antunes, areantunes@yahoo.com.br
Núcleo de Tecnologia, Centro Acadêmico do Agreste-UFPE
Paulo Roberto Maciel Lyra, prmlyra@ufpe.br
Departamento de Engenharia Mecânica, Centro de Tecnologia e Geocências-UFPE
Silvana Maria Afonso Bastos, smb@ufpe.br
Ulisses Porto Filho, uliporto@hotmail.com
Departamento de Engenharia Civil, Centro de Tecnologia e Geociências-UFPE

The analysis of fluid-structure interaction problems involves the modification of the computational domain as the geometry under consideration is moving with time. In several engineering applications, to avoid updating the computational mesh too frequently, an arbitrary Lagrangian Eulerian (ALE) formulation is adopted together with a mesh movement algorithm. In such approach, generally, the reference frame at the moving interface between the structure and the fluid has a Lagrangian description and apart from that has a mixed Lagragian and Eulerian description to accommodate the arbitrary movement of the frame of reference. In this paper, a stabilized finite element method, based on a Fractional Step Method is extended to deal with bidimensional incompressible flow problems with moving boundaries using an ALE formulation. The algorithm adopted to build the dynamic mesh is based on the Modified Laplacian Equation and will be fully described. The structural model considers a simple rigid body with three uncoupled degrees-of-freedom. Some important numerical and implementation issues are also addressed. Finally, the whole system is used to study external flows over a circular cylinder, including the analysis of a fixed cylinder, a moving cylinder with a prescribed forced cross-flow oscillation and a moving cylinder due to the interaction between the fluid and a rigid body. The vortex shedding "lock-in" phenomena is evaluated, which is of great importance for the analysis of vortex induced vibrations (VIV).

Keywords*: Stabilized FEM; Incompressible Navier-Stokes; ALE; Fluid-Structure Interaction*

1. Introduction

Several practical structures, in different engineering fields, are subjected to vibration as a result of flow induced phenomena. Such behavior can compromise the integrity of the structure or make uncomfortable for human use. The analysis of these problems involve the study of a coupled fluid-structure interaction model and can be done using computational modeling. The numerical simulation of such applications is most commonly performed using an interface approach and involves the modification of the computational domain as the geometry under consideration is moving with time. In order to avoid updating the computational discretization too frequently, an arbitrary Lagrangian Eulerian (ALE) formulation (Childs, 1999; Nomura and Hughes, 1992) is normally adopted together with a mesh movement algorithm. In such approach, generally, the reference frame at the moving interface between the structure and the fluid has a Lagrangian description and apart from that has a mixed Lagrangian and Eulerian description to accommodate the arbitrary movement of the frame of reference.

In this paper we briefly describe the finite element procedure developed to simulate the two dimensional fluid-structure interaction of a rigid circular cylinder, immerse in an incompressible viscous fluid flow (Antunes, 2008, Antunes *et al.*, 2009). The analysis of such model application gives insight on many problems of industrial interest, for instance the study of "VIV" (Vortex Induced Vibrations) (Blevins, 1986) on offshore platform legs. The adopted procedure uses a stabilized like Petrov-Galerkin "ALE" (Arbitrary Lagrangian-Eulerian) finite element formulation with Euler time-integration for the fluid-dynamics analysis (Antunes, 2008). This scheme represents an SUPG-like algorithm (Streamline Upwind Petrov-Galerkin (Brooks and Hughes, 1982)) with the Fractional Step Method to stabilize the pressure field. For the structural analysis it uses a simple lumped model with three degrees-of-freedom and the Newmark Method (Hughes, 1987). The fluid-structural coupling is solved through interfacing and implemented in a segregated approach, using an algorithm to control errors due to the existing time delay between the fluid and structural analysis (Blom and Leyland, 1998). Several alternatives for the subdivision of domain into subdomains, where the different descriptions (Eulerian, Lagragian or ALE) are adopted, were incorporated in our computational system. Different types of mesh movement and mesh smoothing were implemented in order to reduce the distortion of the computational meshes over the fluid domain, therefore, in this work we are presenting the most efficient technique found, the Modified Laplacian Equation. The obtained results are in good agreement with the experimental, theoretical and numerical data available in the literature. A preliminary numerical study on the lock-in phenomena is presented. The results show the influence of the amplitude of the displacement of the cylinder on the vortex shedding frequency. Further details and the results for many applications dealing with different levels of difficulty and interaction between

fluid and structure will be analyzed in the future. Finally, we draw the most important conclusions and some on going and future extension of this research.

2. Numerical Formulation

Most fluid structure interaction problems where there is a strong coupling between the displacement of the structure and the flow field are characterized by large displacements of some of the boundaries of the domain. The regions close to these moving boundaries are more naturally discretized with a Lagrangean approach. The fluid regions away from the moving boundaries, however, are more naturally treated with a conventional Eulerian formulation, with a fixed reference frame. We use an Arbitrary Lagrangean Eulerian framework to combine these two approaches in a single numerical technique. The differential equations that described the dynamics of the fluid and the structure therefore must be written in this framework.

2.1. Standard Eulerian Formulation

The flow of incompressible fluids can be described by a specialization of the general Navier-Stokes Equations, where we will also consider that the viscosity is constant and that the fluid is Newtonian. Unless otherwise noted, in the following we will use indicial notation with the summation convention. Within an Eulerian framework, i.e., using a fixed frame of reference and fixed control volumes, the Navier-Stokes equations in non-conservative form reduce to:

$$\rho \frac{\partial u_i}{\partial t} + \rho u_j \frac{\partial u_i}{\partial x_j} = \frac{\partial \tau_{ij}}{\partial x_j} + b_i \tag{1}$$

In the above equation, $i = 1, 2$, x_i are the spatial coordinates, t is the time variable, ρ is the density of the fluid, u_i are the components of the velocity of the fluid, b_i are the external body forces, and τ_{ij} is the stress tensor. Equation (1) is subjected to the incompressibility restriction

$$\frac{\partial u_i}{\partial x_i} = 0; \tag{2}$$

and the stress tensor is given by

$$\tau_{ij} = -p\delta_{ij} + \mu\left(\frac{\partial u_i}{\partial x_j} + \frac{\partial u_j}{\partial x_i}\right) \tag{3}$$

where μ is the dynamic viscosity, p is the pressure and δ_{ij} is Kroenecker's delta. Equations (1), (2) and (3) are written for a fixed geometric domain Ω_f and for a time interval I. For a well posed problem, it is also necessary to impose to the above set of equations boundary conditions on Γ, the boundary of the domain Ω_f, and initial conditions on Ω_f. The boundary conditions are known velocities $\bar{u}$ on Γ_u and known surface tractions $\bar{t}$ on Γ_t, with $\Gamma = \Gamma_u \cup \Gamma_t$ and $\Gamma_u \cap \Gamma_t = 0$. The boundary conditions associated to the mass balance are given in terms of known pressure $\bar{p}$ on Γ_p and known mass flux $\bar{G}$ on Γ_G, with $\Gamma = \Gamma_p \cup \Gamma_G$ and $\Gamma_p \cap \Gamma_G = 0$. Here, $G = \rho u_i n_i$ with n_i being the outward pointing unit normal vector to Γ. The initial conditions are known velocities on Ω_F in the initial time of the analysis.

2.2. ALE Formulation

To develop a finite element discretization applicable to deformable domains, we use an ALE formulation, as proposed in Hughes et al (1981). We define three domains: the spatial domain Ω_Y which is the physical space defined by the material particles at time t; the referential domain Ω_X, which is a fixed domain whose image at time t, subjected to a transformation $\hat{\phi}$, is the spatial domain; and the material domain Ω_Z, which is the domain occupied at the time $t = 0$ by the material particles that occupy the spatial domain at time t. If we define the transformation from the material domain to the spatial domain as ϕ, i.e., $\phi : \Omega_Z \to \Omega_Y$, then the transformation from the material domain to the referential domain is given by $\psi : \Omega_Z \to \Omega_X$, where $\psi = \hat{\phi}^{-1} \circ \phi$ ($\circ$ is the functional composition operator). Now let

us consider that z_i and x_i represent particles in Ω_Z and Ω_X whose image at time t is y_i in Ω_Y. Therefore, considering the transformation ϕ, we can write that:

$$u_i = y_i - z_i, \qquad \dot{u}_i = \dot{y}_i \qquad \text{and} \qquad y_{i\cdot j} = \frac{\partial y_i}{\partial z_j}, \tag{4}$$

where u_i is the displacement, $\dot{u}_i$ is the velocity and $y_{i\cdot j}$ is the deformation gradient. In a similar manner, considering the transformation $\hat{\phi}$, we can write:

$$\hat{u}_i = y_i - x_i, \qquad \hat{u}_i' = y_i' \qquad \text{and} \qquad y_{i\acute{j}} = \frac{\partial y_i}{\partial x_j}, \tag{5}$$

where $\hat{u}_i$ is the displacement, $\hat{u}_i'$ is the velocity and $y_{i\acute{j}}$ is the deformation gradient. Finally, considering the transformation ψ, we can write:

$$w_i = x_i - z_i, \qquad \dot{w}_i = \dot{x}_i \qquad \text{and} \qquad x_{i\cdot j} = \frac{\partial x_i}{\partial y_j}, \tag{6}$$

where w_i is the displacement, $\dot{w}_i$ is the velocity and $y_{i\cdot j}$ is the deformation gradient. Equations (4) to (6) are the kinematic relationships for the different descriptions of a continuum.

With the above mappings, we can write (Antunes *et al.*, 2005) that:

$$c_i = \dot{u}_i - \hat{u}_i' = \frac{\partial y_i}{\partial x_j}\frac{\partial x_j}{\partial t} \tag{7}$$

where c_i is defined as the convective velocity. If f is a scalar function of the flow field, the material derivative of this function is given by (Childs, 1999):

$$\frac{Df}{Dt} = \frac{\partial f}{\partial t} + \frac{\partial f}{\partial x}F^{-1}c \tag{8}$$

where $F_{ij} = \frac{\partial y_i}{\partial x_j}$ is the deformation gradient between the reference and the spatial domain, and c_i is the convective velocity defined in Eq. (7). In this work, we used a single step Crank-Nicholson scheme for the time integration, therefore throughout the duration of each and every time step, the referential and spatial domains are coincident. The deformation gradient between these two domains is the identity transformation, so Eq. (8) reduces to:

$$\frac{Df}{Dt} = \frac{\partial f}{\partial t} + \frac{\partial f}{\partial x}c \tag{9}$$

It is well worth noting that if $\hat{u}_i' = 0$ in Eq. (7), we have the conventional Eulerian description, and if $\hat{u}_i' = \dot{u}_i$, we have the Lagrangean description. With this definition of the material derivative, the incompressible Navier-Stokes equations in the ALE formulation reduce to:

$$\rho\frac{\partial u_i}{\partial t} + \rho c_j\frac{\partial u_i}{\partial x_j} = \frac{\partial \tau_{ij}}{\partial x_j} + b_i \tag{10}$$

2.3. Finite Element Discretization

The incompressible Navier-Stokes Equations Eqs.(1-2) can be write, in an ALE description, without thermal effects, in continuous form can be written like:

$$\frac{\partial \mathbf{u}}{\partial t} + (\mathbf{c}\cdot\nabla)\mathbf{u} - \upsilon\Delta\mathbf{u} + \nabla p = \mathbf{f} \quad \text{in } \Omega\times(0,t) \tag{11}$$

$$\nabla\cdot\mathbf{u} = 0 \qquad \text{in } \Omega\times(0,t) \tag{12}$$

where Ω is the spatial fluid domain, t is the time variable, (0,t) is the time interval, $\mathbf{u}$ is the velocity field, υ is the kinematic viscosity, p is the pressure, $\mathbf{f}$ is the external force vector, ∇ is the gradient operator and Δ is the Laplacian operator, and $\mathbf{c}$ is the convective velocity field. The physical boundary was divided in two non-overlapping parts Γ_{du} and Γ_{nu} in which the Dirichlet and Neuman boundary conditions are prescribed to each equation, respectively. The Dirichlet and Neuman boundary conditions are:

$$\mathbf{u} = \bar{\mathbf{u}} \quad \text{in } \Gamma_{du}, \qquad p = \bar{p} \quad \text{and} \qquad \mathbf{n}\cdot\boldsymbol{\sigma} = \bar{\mathbf{t}} \quad \text{in } \Gamma_{nu} \tag{13}$$

where $\boldsymbol{\sigma}$ is the viscous stress tensor, $\mathbf{n}$ is the unit outward normal vector, and $\bar{t}$ is the surface stress or traction. An upper bar refers to a prescribed value. Finally, initial conditions must be known in the whole domain at the initial time.

In this work, a Fractional Step method based in a LU factorization (Antunes, 2008, Antunes *et al.,* 2009, Codina, 2002, Chang *et al.,* 2002, Henriksen *et al.*, 2002) was applied. In this method the final system is analogous to the method proposed by Chorin in 1967, and Temam in 1969, that applies Helmholtz decomposition. The final discrete system is obtained by using a θ method in time, resulting in a trapezoidal discretization, and a Finite Element Method for the spatial discretization (Gresho *et al.*, 1998, vols. 1 & 2, Zienkiewicz ant Taylor, 1988). The stabilization of the advective and the gradient pressure terms are obtained with an orthogonal projection of these terms in a finite element space (Codina, 2000, Codina, 2002, Soto *et al.*, 2001). The discrete variational formulation (Soto *et al*., 2001, Soto *et al*., 2004) can be written as: knowing $\mathbf{u}_h^n$ and p_h^n, find $\left(\mathbf{u}_h^{n+1}, p_h^{n+1}, \boldsymbol{\pi}_h^{n+1}, \xi_h^{n+1}\right)$ in $\mathbf{V}_h\times\mathbf{Q}_h\times\tilde{\mathbf{V}}_h\times\tilde{\mathbf{V}}_h$, such that:

$$\frac{1}{\delta t}\left(\mathbf{u}_h^{n+1,i} - \mathbf{u}_h^n, v_h\right) + \left(\mathbf{c}_h^{n+1,i-1}\cdot\nabla\mathbf{u}_h^{n+\theta,i}, v_h\right) + \left(\upsilon\nabla\mathbf{u}_h^{n+\theta,i}, \nabla v_h\right) - \left(p_h^{n+1,i-1}, \nabla\cdot v_h\right)$$
$$+\left(\tau\left(\mathbf{c}_h^{n+\theta,i-1}\cdot\nabla\mathbf{u}_h^{n+\theta,i} - \beta^{n+1,i-1}\boldsymbol{\pi}_h^{n+\theta,i-1}\right), \mathbf{u}_h^{n+\theta,i-1}\cdot\nabla v_h\right) = \left(\mathbf{f}^{n+\theta}, v_h\right) + \left(\boldsymbol{\sigma}^{n+\theta,i-1}\cdot\mathbf{n}, v_h\right)_{\Gamma_{nu}} \tag{14}$$

$$\delta t\left(\nabla p_h^{n+1,i} - \nabla p_h^{n+1,i-1}, \nabla q_h\right) + \left(\tau\left(\nabla p_h^{n+1,i} - \beta^{n+1,i-1}\xi_h^{n+1,i-1}\right), \nabla q_h\right) = -\left(\nabla\cdot\mathbf{u}_h^{n+1,i}, q_h\right) \tag{15}$$

$$\left(\boldsymbol{\pi}_h^{n+\theta,i}, \tilde{v}_h\right) = \left(\mathbf{c}_h^{n+\theta,i}\cdot\nabla\mathbf{u}_h^{n+\theta,i}, \tilde{v}_h\right) \tag{16}$$

$$\left(\xi_h^{n+1,i}, \tilde{v}_h\right) = \left(\nabla p_h^{n+1,i}, \tilde{v}_h\right) \tag{17}$$

$$\forall\left(v_h, q_h, \tilde{v}_h, \tilde{v}_h\right) \in \mathbf{V}_h\times Q_h\times\tilde{\mathbf{V}}_h\times\tilde{\mathbf{V}}_h$$

where $\mathbf{u}_h^{n+1}, p_h^{n+1}, \boldsymbol{\pi}_h^{n+1}, \boldsymbol{\xi}_h^{n+1}$ are the velocity vector, pressure, advective projection term and pressure gradient projection term, respectively, and $\mathbf{V}_h\times\mathbf{Q}_h\times\tilde{\mathbf{V}}_h\times\tilde{\mathbf{V}}_h$ are the corresponding finite element functional spaces, respectively. The superscripts n and i refer to time step and Gauss-Seidel iterations counter in each time step, the subscript h refers to discrete variables, δt is the size of the time step, β is the stabilization parameter based on pressure gradient, limited to the interval I=[0 1], taking values close to 1 where the pressure field is smooth and close to 0 in flow regions with sharp pressure gradients (Soto *et. al.*, 2004), τ is the stability and convergence parameter, θ is the time integration parameter (for instance θ = 1.0 implies Backward Euler and θ = 0.5 Crank-Nicholson), v_h, $\tilde{\mathcal{V}}_h$, q_h, are the finite element weight functions to velocity, advective and pressure gradient projections and pressure, respectively. The variables $\boldsymbol{\pi}$ and $\boldsymbol{\xi}$ were obtained by LU factorization of the system. The functional form $(\cdot,\cdot)$, is defined by:

$$(a,b)=\int_{\Omega} a\cdot b d\Omega\,,\ (a,b)_{\Gamma}=\int_{\Gamma} a\cdot b d\Gamma \tag{18}$$

2.4. Edge Based Data Structure

We are using an edge based data structure, which is advantageous in terms of CPU time, because most of the discrete terms do not need to be re-computed at each iteration by looping through the elements. The local conservation and symmetry are enforced at the discrete level calculating only the non-diagonal terms and by computing the diagonal one as the negative value of the summation of the same-row non-diagonal terms (Soto *et al.*, 2004). The final edge based terms are obtained replacing the standard loop over the elements to edge loops. To exemplify, consider the first term of the Eq. (15), which has diffusive transport character, and eliminating sub/super-index, yields:

$$(\nabla p,\nabla N)=\int_{\Omega}\nabla p\cdot\nabla N d\Omega=\sum_{E\supset J}\int_{\Omega_E}\nabla N_I\cdot\nabla N_J d\Omega_E\,\hat{p}_J=$$
$$\sum_{S=1}^{m}\left\{\sum_{E\supset IJ}\int_{\Omega_E}\left(\sum_{k=1}^{n\dim}\frac{\partial N_I}{\partial x_k}\frac{\partial N_J}{\partial x_k}\right)d\Omega_E\right\}(\hat{p}_I-\hat{p}_J)=\sum_{S=1}^{m}C_{IJ}(\hat{p}_I-\hat{p}_J) \tag{19}$$

where the Galerkin formulation (i.e. the same weighting and shape function N) is adopted, and C_{IJ} is a coefficient associated to edge *IJ*.

Observe that the final term of Eq. (19) is naturally conservative, meaning that the diffusive transport from node *I* to node *J* is equal to the diffusive transport from node *J* to node *I*.

2.5. Structural Dynamics

In this work we only consider dynamics of rigid bodies. The movement of the body is obtained with a straightforward application of Newmark's Method (Hughes, 1987, Antunes *et al.*, 2005):

$$\mathbf{M}\mathbf{a}^{t+\Delta t}+\mathbf{C}\mathbf{v}^{t+\Delta t}+\mathbf{K}\mathbf{d}^{t+\Delta t}=\mathbf{F}^{t+\Delta t} \tag{20}$$

$$\mathbf{v}^{t+\Delta t}=\mathbf{v}^{t}+\left[(1-\gamma)\mathbf{a}^{t}+\gamma\mathbf{a}^{t+\Delta t}\right]\Delta t \tag{21}$$

$$\mathbf{d}^{t+\Delta t}=\mathbf{d}^{t}+\mathbf{v}^{t}\Delta t+\left[\left(\frac{1}{2}-\beta\right)\mathbf{a}^{t}+\beta\mathbf{a}^{t+\Delta t}\right]\Delta t^{2} \tag{22}$$

where **d**, **v**, and **a** are the displacements, velocity and acceleration of the body, and β and γ are parameters of the method, and **M**, **C**, and **K** are the mass, damping and stiffness matrices of the structure. In this work we used $\gamma=1/2$ and $\beta=1/4$, which leads to an implicit, second order accurate and unconditionally stable time integration scheme. The stability of this scheme is important because the time step increment for the structural time evolution is taken as the same as the time increment chosen for the CFD solution. This time increment is determined by the stability requirements of the CFD algorithm, and therefore its time scale is completely unrelated to the dynamic behavior of the structure.

2.6. Fluid Structural Coupling

The coupling between the fluid and structural field was imposed in a segregated manner, and compatibility conditions are imposed a posteriori, at the end of each time step, to enforce the consistency of the interface between both fields. This approach has the advantage, in contrast to a monolithic approach, that the most efficient numerical solution technique can be used for each particular field.

At the start of each time step, we assume that the interfaces are consistent, i.e., that points lying on the interface between the structural and fluid domain have the same velocities, when considered belonging to either domain. Each domain is then advanced in time independently, according to its own physics. The other domain is considered static, and used only as a source of initial and boundary conditions for the current time step. At the end of the time step, the interfaces will therefore no longer be consistent, so in fact a series of predictor-corrector steps is repeated until satisfactory agreement between the two fields is reached. As the interfaces between domains move along the time, the mesh is distorted by the movement of the boundaries of the domain, and when this distortion becomes excessive, the

inadequate elements are removed and the mesh is recreated in these regions. The predictor-corrector technique adopted is adapted from the one proposed by Bloom et al. (1998), and the general procedure is summarized below:

a. For all time step do:
b. Estimate a predictor velocity Vp
c. Move structure and mesh in the computational domain
d. Solve the CFD problem
e. Solve the structural dynamics problem
f. Compute a corrector velocity Vc
g. If Vp and Vc converged to each other, then:
h. Advance to next time step
i. Else:
m. Vp = Vc
n. Repeat from step c

The predictor velocity Vp at the start of each time increment (step b) is taken as an estimate of the current velocity of the structure. This velocity is computed by a simple linear extrapolation from the structural velocity and acceleration computed at the previous time step. As the interpolation of solutions between meshes (step f) is not cheap and can introduce errors, we try to minimize it by restricting the regions where the mesh is allowed to move. This will be described further below. The CFD solution (step d) uses as boundary conditions for the moving boundaries the current velocity of the interface, Vp. The corrector velocity Vc (step f) is the interface velocity that results from the solution of the structural dynamics problem (step e). The convergence test (step g) verifies if the difference between the corrector velocity Vc and Vp are less than some prescribed tolerance. If this is so, the algorithm advances to the next time step (step h), otherwise the current corrector velocity is taken as the new predictor velocity and the predictor-corrector loop is repeated. In this work we only dealt with rigid bodies, therefore the velocity of the interface nodes can be easily computed from the velocity of body with simple transformation matrices (Nomura and Hughes, 1992).

3. Numerical Tools

There are many practical aspects to a successful computational implementation of the procedures described above. Clearly, facilities for dealing with deformable domains, which involve automatic mesh generation, assessment of mesh quality, and automatic mesh movement are all important aspects. The most interesting aspects of our implementation will be described below.

3.1. Subdomain partitioning

The partition of a domain into simpler subdomains is a well proven practical technique that helps the mesh generation in domains with complex geometry. Is this work, this idea is extended and different numerical formulations can be employed for the discretization on each subdomain. We have implemented three distinct possibilities: a conventional Eulerian formulation, an ALE formulation with a deformable mesh and an ALE formulation where the mesh is movable but not deformable. The Eulerian formulation is more appropriate for regions of fluid away from the moving boundaries. The ALE formulation with non-deformable but moving meshes is used in the regions very close to the moving interfaces. These meshes are attached to the moving bodies, and are not deformable because, in general, complex flow phenomena that require very fine and high quality meshes, such as boundary layer formation or separation bubbles, occur in these regions. Deformation of the mesh would quickly destroy the quality of these meshes and compromise the quality of the solution. The ALE formulation with deformable meshes is used to couple the two kinds of domains just described. A simple sketch example can be seen in Fig. (1). For the structure, of course, we use a Lagrangian decription.

The use of different formulations for different subdomains is important because it minimizes the needed interpolation of solutions between different meshes. Clearly, in the subdomains where an Eulerian formulation is used, the interpolation is completely unnecessary because the mesh never varies. Interpolation between unstructured meshes, even with the use of adequate data structures to speed up searches, is a somewhat costly procedure. The interpolation can also reduce the accuracy of the numerical solution, therefore it is important that it be restricted to the as small a region as possible. In the current implementation, the subdomain decomposition and the assignment of formulations is done a priori by the user, therefore some knowledge of the expected amplitudes of displacement is necessary. In practice, however, this has not proven itself to be a problem.

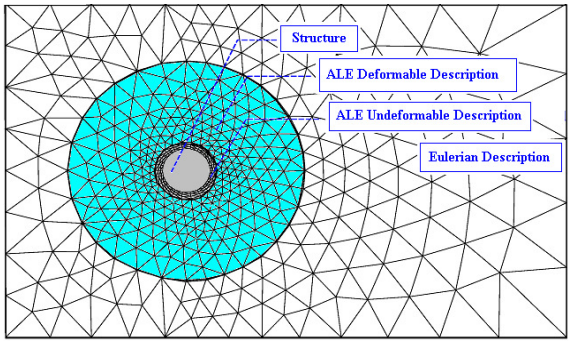

Figure 1. Computational model: subdomain decomposition and differents descriptions.

3.2. Mesh Movement

In the domains with a deformable ALE formulation, the movement of the interface nodes causes distortions of the original shapes of the elements connected to these nodes.

In order to avoid excessive elements distortion, in this work we are solving a modified Laplace equation for the mesh domain. The diffusivity coefficient is based on volume of the elements, and is designed to smooth the distortions caused by structure displacements (Kanchi and Massud, 2007, Liberato *et al.*, 2010).

The domain is divided as follow: Ω is the domain of the equation, Γ_m is the moving boundary (structure surface), and Γ_f is the fixed domain. So the classical formulation of the problem results: given **v** on the boundaries, find **v** in the domain, such that

$$\nabla \cdot \left(\left[1 + \tau \right] \nabla \right) \mathbf{v} = 0 \tag{23}$$

$$\mathbf{v} = \mathbf{v_0} \text{ in } \Gamma_m \tag{24}$$

$$\mathbf{v} = \mathbf{0} \text{ in } \Gamma_f \tag{25}$$

where $\Gamma = \Gamma_m \cup \Gamma_m$, and **v**, the displacement vector, and is need to solve the equation for each direction.

Note that the diffusivity coefficient must be defined in order to the smaller elements, generally defined close of the structure, where the small scale effects are presents, they are suffering minimum deformations. This way, the displacements are sent through the mesh until the bigger elements, close to the boundaries, can be smooth the displacements. Kanchi e Masud, 2007, propose the calculus of the coefficient to avoid excessive deformations providing aditional subjects for the elements. The coefficient used by Kanchi and Massud, 2007, in the Eq. (23), and used in this work is;

$$\tau^e = \frac{1 - V_{\min} / V_{\max}}{V^e / V_{\max}} \tag{26}$$

where $V_{\min}$ = minimum volume of the mesh element, $V_{\max}$ = maximum volume of the mesh element, V^e = volume of the element.

4. Applications

The scheme above described has already been utilized for the simulation of a variety of applications (Antunes, 2008, Antunes *et al.*, 2009, Liberato *et al.*, 2010), involving stationary and/or moving boundaries, including the study of the flow around a fixed cylinder, the flow around a cylinder with an imposed periodic displacement, the free vibration of the cylinder in a stationary fluid and the next step of this work is to analyze the coupled fluid-structure problem of the vortex inducing vibrations on a rigid cylinder. In this work we are interested to obtain the lock-in phenomena conditions.

4.1 Vortex "Lock-in" Regime Under Forced Oscillating Cylinder

The numerical procedure described is used to simulate the external flow over a moving cylinder with a prescribed forced cross-flow oscillation, for several different Reynolds number. A detailed description of the computational domain with boundary and initial conditions can be seen in the Fig. 7.

The follow boundary conditions are applied in this example: non-slip condition on the surface of the rigid body; uniform velocity field with $u_1 = u^0$ e $u_2 = 0$ is prescribed in the inflow face; for the below and above faces the boundary condition are $u_2 = 0$ e $t_1 = 0$; on the outflow boundary , the pressure value is prescribed, with p = 0 and traction free condition, e.g., $t_1 = t_2 = 0$. The initial condition is the velocity field with the components $u_1 = u^0$, $u_2 = 0$ which are specified over the all the domain in the initial time $t = t^0$, and a referential pressure $p = 0$. In this notation, the boundary condition traction is represented by "t_i", where the subscript i, represents the directions of application, and the time is represented by "t^n", ,where the superscript n represents the level time. The vertex of the domain are (-5,-5), (-5,5), (10,-5) e (10,5), and the circular cylinder have a unitary diameter and is centered on the origin of the orthogonal coordinates.

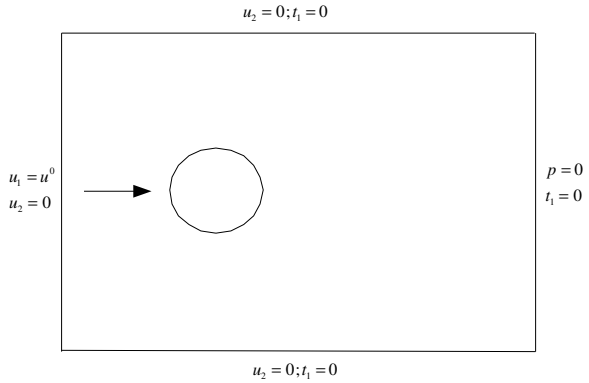

Figure 7. Description of domain for the lock-in applications.

By computing the fluid flow considering a fixed cylinder we obtain the variation of the frequency of the vortex shedding at different Reynolds number, Re. The computed frequencies of the vortex shedding, presented in the first column of Table 1, agree with the experimental data (Blevins, 1986).

The "lock-in" phenomena (Blevins, 1986) occurs when the response frequency of the cylinder synchronises with the vortex shedding frequency. By imposing an harmonic oscillation to the cylinder and by analysing the modification on the vortex shedding frequency such phenomena can be studied. Taking the vortex shedding frequency obtained with the analysis of a fixed cylinder at Re=120 (0,1613 Hz) as the forced frequency imposed to the cylinder, varying the Reynolds number from 100 to 140 and the amplitude ratio (Ay/D) from 0% to 8% we built the Table 1. This table show the influence of the amplitude of the forced displacement on the vortex shedding frequency. The flow regime are "locked-in", i.e. the displacement and vortex shedding are in phase, for all values of Reynolds number and displacement amplitude ratio presented in the table with bold numbers. Whenever the vortex shedding frequency is different from the one obtained with a fixed cylinder we say that it is in a "perturbed" regime, and when the imposed movement does not change the vortex shedding frequency, the regime is unperturbed and out of "lock-in". Our results are in good agreement with that presented in the literature (Blevins, 1986, Correia, 2001). By increasing the displacement ration to 2% we get a perturbed regime, and then a "lock-in" regime for all Reynolds number analysed, for 3,5% and 5%. If we increase the amplitude ratio to 8% the flow gets out of the "lock-in" regime for most Reynolds number..

The harmonic function to displace the cylinder adopted is

$$Y(t) = a \sin\left(2\pi f \left(t - t^0 \right)^n \right) \tag{37}$$

where, a is the amplitude displacement, f is the frequency, and t^0 is the initial time. In this work $t^0 = 0$, $n = 1$, $f = 0{,}1613$ Hz and a varying.

For such Reynolds number and amplitude of oscillation the flow is initially perturbed by the oscillation of the cylinder and later the "lock-in" phenomena is established. This can be further observed in Figure 8, which shows the transversal velocity (Uy) and the relative displacement amplitude.

Table 1. Displacement ratio influence to obtain "lock-in" for different Reynolds numbers.

Re	**Displacement Ratio (Ay/D)**				
	0,0%	2,0%	3,5%	5,0%	8,0%
100	0.1412	**0.1613**	**0.1613**	**0.1613**	0.1618
120	**0.1613**	**0.1613**	**0.1613**	**0.1613**	**0.1613**
140	0.1634	0.1618	0.1618	**0.1613**	0.1615

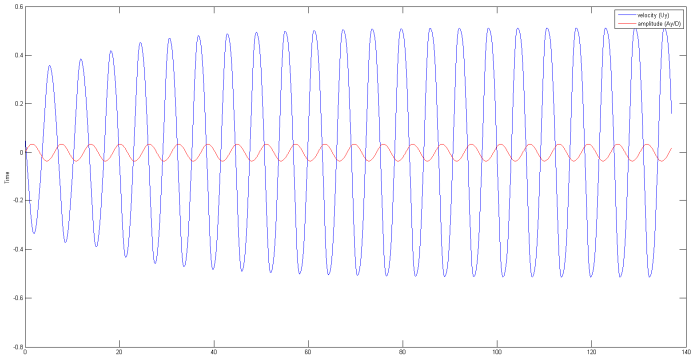

Figure 8. Velocity and Amplitude of oscillation, regime under forced transverse oscillation, Ay/D = 3.5% at Re=100.

A contour plot of the computed pressure can be seen in Figure 9, where the Von Karman vortex street behind the cylinder is characterized, for the flow at Re=120.

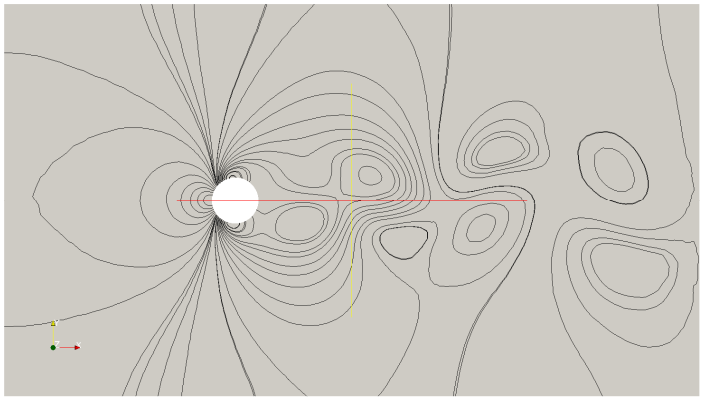

Figure 9. Pressure isolines.

5. Conclusions

A brief description of the developed computational system for fluid-structure interaction analysis was presented. Such system incorporates several important tools (different mesh movement algorithms; possibility to decompose the domain into several subdomains with different reference frame description) which renders it's very flexible and capable to deal with a large class of two dimensional applications. Some of these tools and strategies were not exploited in this application and must also be tested with more complex problems to stress their real importance. The results obtained through the study of the lock-in phenomena on a circular cylinder are qualitatively consistent with the literature, however they are just preliminary and requires further investigation. A monolithic implicit FEM formulation has been presented to solve Navier-Stokes equations for laminar incompressible tridimensional flows. The formulation also includes stability properties for pressure and convection and a Fractional Step procedure. An edge-based data structure was used to assembly all global matrices involved in the computational model. The implicit formulation presented is very attractive for the analysis of transient problems in which the time step can assume larger values than those required for explicit formulation, which are severely restricted by stability criteria.

Finally, other improvements are required in terms of efficiency to allow the analysis of large-scale problems within an acceptable time. This improvements would involve, for instance, the incorporation of an error estimator to control the adaptive procedure, a parallel or parallel/vector implementation and others elements of high performance computation. Some of this aspects are already under investigation.

6. Acknowledgement

The authors would like to thank the Brazilian Government, through the Agencies FACEPE, CAPES, CNPq and MCT-ANP for the financial support provided.

7. References

Antunes, A. R. E., Carvalho, D. K. E., and Lyra, P. R. M., 2002, "Different Strategies for Mesh Movement and Remeshing of Unstructured Meshes Used When Dealing with Fluid-Structure Interaction Problem", 9th Brazilian Congress of Thermal Engineering and Science, Caxambu, Brasil (in Portuguese and in CD-ROM).

Antunes, A. R. E., Lyra, P. R. M., Willmersdorf, R. B., 2005, "A Methodology and Computational System for the Simulation of Fluid-Structure Interaction Problem". J. of the Braz. Soc. Of mech. Sci. & Eng., Vol. XXVII, No.3, p. 255-265.

Antunes, A. R. E., 2008, "Um Sistema Computacional Utilizando uma Formulação do Tipo Fractional Step e o Método dos Elementos Finitos por Arestas para a Análise de Escoamentos Incompressíveis 3D Usando Computação Paralela", D.Sc. Thesis, Recife, Brazil (*in Portuguese*).

Antunes, A. R. E., Lyra, P R. M., Da Silva, R. S., Wilmmersdorf, R. B., 2009, "An Implicit Monolithic Finite Element to Solve 3D Incompressible Navier-Stokes Equations using Fractional Step Method and Parallel Edge-Based Implementation", 20th International Congress of Mechanical Engineering, Gramado, RS, Brazil, 10p.

Blevins, R. D., 1986, "Flow-Induced Vibration", R. E. Krieger Publishing, Inc, Malabar/Florida, USA, 363 p.

Blom, J. F. and Leyland, P., 1998, "Consistency Analysis of Fluid-Structure Interaction Algorithms", European Cong. on Comp. Methods in App. Science and Eng. (ECCOMAS), Barcelona, Spain, 15 p. (in CD-ROM).

Brooks, A. N. and Hughes, T. J. R., 1982, "Streamline Upwind/Petrov-Galerkin Formulations for Convection Dominated Flows with Particular Emphasis on the Incompressible Navier-Stokes Equations", Computer Methods in Applied Mechanics and Engineering, Vol. 32, pp. 199-259.

Chang, W., Giraldo, F., Perot, B., 2002, Analysis of an exact fractional step method, J. Computational Physics, vol. 180, p. 183-199.

Childs, S. J., 1999, "The Energetic Implications of Using Deforming Reference Descriptions to Simulate the Motion of Incompressible Newtonian Fluids", Computer Methods in Applied Mechanics and Eng., vol. 180, pp 219-238.

Chorin, A. J., 1967, "A Numerical Method for Solving Incompressible Viscous Problem", J. Comput. Phys., vol. 2.

Codina, R., 2000. "Stabilization of incompressibility and convection trough orthogonal sub-scales in finite element methods", Compt. Meth. Applied Mechanics and Engineering, v. 190, p. 1579-1599.

Codina, R., 2002. "Stabilized finite element approximation of transient incompressible flows using orthogonal subscales", Comp. Meth. Applied mechanics and Engineering, vol 191, p. 4295-4321.

Correia, A.C.A., "2001, Simulações Computacionais da Formação de Vórtices em um Cilindro com Ênfase na Vibração Induzida por Vórtice", Recife, 67p M.Sc. Thesis, Recife, Brazil (*in Portuguese*).

Gresho, P. M., Sani, R. L., 1998. Incompressible flow and the finite element method, John Wiley & Sons, vol. 2.

Henriksen, M. O., Holmen, J., 2002. Algebraic splitting for incompressible Navier-Stokes equations, J. Computational Physics, vol. 175, p. 438-453.

Hughes, T.J.R., Liu, W.K. and Zimmermann, T.K., 1981, "Lagrangian-Eulerian Fomulation for Incompressible Viscous Flows", Computer Methods in Applied Mechanics and Engineering, vol. 29, pp. 329-349.

Hughes, T. J. R., 1987, "The Finite Element Method", 1ª Edition, United States of America, Prentice-Hall, Inc., 803p.

Kanchi, H., & Masud, A., 2007, "A 3D adaptive mesh moving scheme", Int. Journal for Num. Meth. In Fluids, vol 54, pp 923-944.

Liberato, B. E., Antunes, A. R. E., Lyra, P. R. M., 2010, " Usando a Equação de Laplace e o Método dos Elementos Finitos para a Suavização de Malhas em Problemas de Interação Fluido-Estrutura", VI National Congress of Mechanical Engineering, Campina Grande, PB, Brazil, 11p, (*in Portuguese*).

Nomura, T. and Hughes, T.J.R., 1992, "An Arbitrary Lagrangian-Eulerian Finite Element Method for Interaction of Fluid and a Rigid Body", Computer Methods in Applied Mechanics and Engineering, vol. 95, pp. 115-138.

Soto, O., Löhner, R. and Cebral, J., 2001, "An implicit monolithic time accurate finite element scheme for incompressible flow problems", In: 15th AIAA Computational Fluid Dynamics Conference, Anaheim, EUA, June.

Soto, O., Löhner. R., Cebral, J. and Camelli, F. 2004. "A stabilized edge-based implicit incompressible flow formulation", Comp. Meth. Applied Mechanics and Engineering, vol. 193, p. 2139-2154.

Temam, R., 1969, "Sur l'approximation de la solution des équaciones de Navier-Stokes par la méthode dês pás fractionaires (I)", Arch. Ration. Mech. Anal., vol. 32 (*in French*).

Zienkiewicz, O. C., Taylor, R. L., 1988, "The finite element method: basic formulation and linear problems", vol 1, MacGraw-Hill, 4ª edition.

8. RESPONSIBILITY NOTICE

The authors are the only responsible for the printed material included in this paper.